



Contents lists available at ScienceDirect

Bioorganic & Medicinal Chemistry Letters

journal homepage: www.elsevier.com/locate/bmcl

Effect of novel *N*-cyano-tetrahydro-pyridazine compounds, a class of cathepsin K inhibitors, on the bone resorptive activity of mature osteoclasts

Seong Hwan Kim^a, Dong Joo Jhon^b, Jong Hwan Song^b, Jae Sung No^b, Nam Sook Kang^{c,*}^a Laboratory of Chemical Genomics, Korea Research Institute of Chemical Technology, PO Box 107, Yuseong-gu, Daejeon 305-600, Republic of Korea^b Center for Medicinal Chemistry, Korea Research Institute of Chemical Technology, PO Box 107, Yuseong-gu, Daejeon 305-600, Republic of Korea^c Laboratory of Computer-aided Molecular Design, Korea Research Institute of Chemical Technology, PO Box 107, Yuseong-gu, Daejeon 305-600, Republic of Korea

ARTICLE INFO

Article history:

Received 21 May 2008

Accepted 3 June 2008

Available online 10 June 2008

Keywords:

Cathepsin K

Osteoclast

Docking

Inhibitor

Bone resorption

ABSTRACT

Cathepsin K is the key regulator in the osteoclast-mediated bone resorption. Here, we found the correlation between the inhibitory activities of carbonitrile derivatives in the enzymatic activity of cathepsin K and their binding scores predicted using FlexX-Pharm docking program. The binding pattern of [1-(2-cyano-tetrahydro-pyridazine-1-carbonyl)-2-methy-propyl]-carbamic acid benzyl ester (**8**), one member of this series, was similar to that of the reference. In a bone pit formation assay, compound **8** was shown to dose-dependently inhibit the bone resorptive activity of mature osteoclasts.

© 2008 Elsevier Ltd. All rights reserved.

Bone mass is maintained through bone remodeling in which old bone is removed from skeleton by osteoclasts and new bone added through the process of mineralization by osteoblasts.¹ However, an imbalance in bone remodeling that is caused by increased bone resorption over bone formation leads to most skeletal diseases including osteoporosis. The development and progress of osteoporosis then increase the risk for fractures (particularly in the hip) that are a serious problem with many adverse consequences such as substantial skeletal deformity, pain, functional limitation, increased mortality, and severe economic burden.²

The attachment of osteoclasts to bone surface triggers osteoclast-mediated bone resorption. After attaching to the bone surface, a tightly sealed resorption lacuna is created and then several proteolytic enzymes expressed in osteoclasts are secreted into the lacuna for the removal of bone mineral and the degradation of organic matrix proteins.³

Interestingly, cathepsin K is the most abundant cysteine protease expressed in osteoclasts and capable of degrading type I collagen, the major component of bone matrix.⁴ The finding of cathepsin K deficiency in pycnodysostosis, an osteopetrotic disorder characterized by decreased bone resorption, further underscores the importance of cathepsin K as a potential target for developing agents to treat osteoporosis and other disorders characterized by increased bone resorption.⁵

In a previous study, researchers in GlaxoSmithKline and Merck/Celera had reported the discovery of cathepsin K inhibitors based on cyanamide (Fig. 1).⁶ These observations prompted us to explore new cathepsin K inhibitors that possess the *N*-cyano-tetrahydro-pyridazine structure (Fig. 2). Therefore, in this study, we evaluated the activity of derivatives of novel *N*-cyano-tetrahydro-

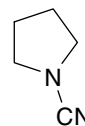


Figure 1. The cyanamide structure as the main pharmacophore of cathepsin K inhibitors.

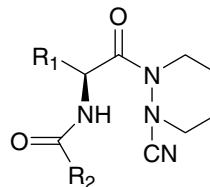
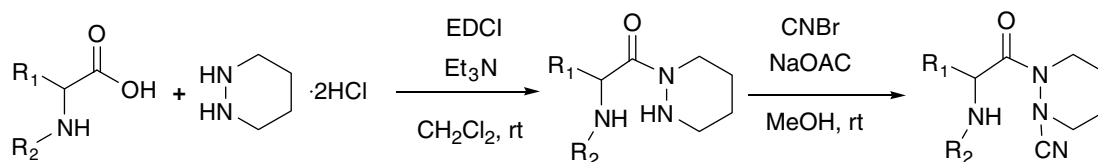


Figure 2. The core structure of new cathepsin K inhibitors containing *N*-cyano-tetrahydro-pyridazine.

* Corresponding author. Tel.: +82 42 860 7452; fax: +82 42 860 7635.

E-mail address: nskang@kriict.re.kr (N.S. Kang).



Scheme 1. Reagents and conditions.

pyridazine compounds as cathepsin K inhibitor, and analyzed their interaction pattern with cathepsin K using the commercial docking program.

A series of novel *N*-cyano-tetrahydro-pyridazine derivatives were selected using docking study and synthesized as shown in Scheme 1. Coupling amino acids with tetrahydropyridazine using EDCI in the presence of triethylamine, and subsequent *N*-cyanation of the tetrahydro-pyridazine moiety by the addition of cyanogen bromide and sodium acetate led to the *N*-cyano-tetrahydro-pyridazine amino acid derivatives.⁷

In the following experiment, the inhibitory activities of *N*-cyano-tetrahydro-pyridazine derivatives (**1–8**) were evaluated by using in vitro enzymatic activity assay for cathepsin K as well as cathepsin B and L that are also lysosomal acid cysteine proteases located in osteoclastic resorption lacunae. Most of compounds showed strong inhibitory activities for cathepsin K (Table 1) and interestingly, compound **8** with strongest inhibitory activity for cathepsin K in tested compounds was shown to have the specificity for cathepsin K ($IC_{50} = 1$ nM); its inhibitory activities for cathepsin B and L were 10 to 145 times less than that for cathepsin K.

For docking of *N*-cyano-tetrahydro-pyridazine derivatives (**1–8**), 1YK7.pdb^{6b} was used as a reference complex structure. In addition, the binding score value was calculated using Sybyl7.1/ChemScore⁸ method with relax molecule algorithm. As shown in Figure 3, the good binding model showing a high correlation ($R^2 = 0.8$) between the binding score (ChemScore) and the inhibitory activity was obtained. The binding pattern of compound **8**, which was the most potent cathepsin K inhibitor, as predicted, was very similar to the reference complex structure (Fig. 4), keeping important interactions with cathepsin K as reported in other researcher's studies.⁶

In the next experiment, the effect of compound **8** on the bone resorptive activity of mature osteoclasts was evaluated by using both RAW264.7 cells and mouse bone marrow-derived macrophages (BMMs).⁹ The receptor activator of nuclear factor κ B (NF- κ B) ligand (RANKL)-induced mature osteoclasts resorbed bone matrices, but the whole area of resorption pit

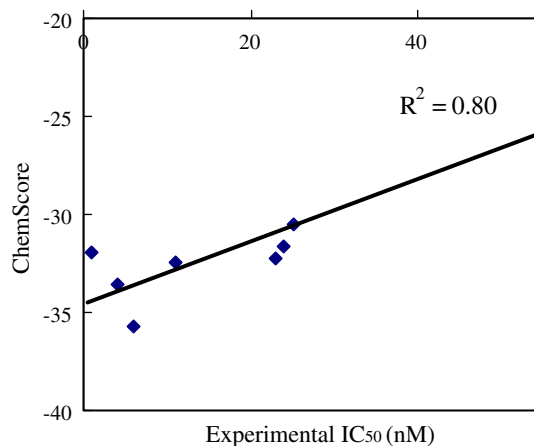


Figure 3. The correlation plot of experimental IC_{50} versus ChemScore values obtained from docking study.

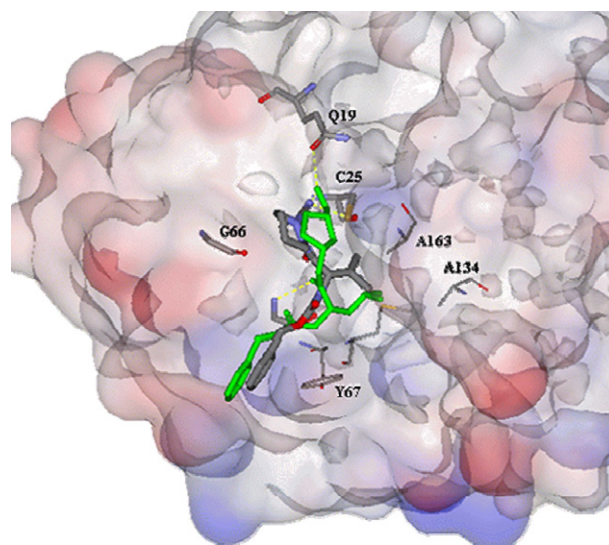


Figure 4. Compound **8** (gray element color) is docked in the active site of the known crystal structure deposited in the Brookhaven Protein Data Bank, 1YK7. Compound shown with green color is the complexed original ligand in 1YK7. This figure was generated using Accelrys Discovery Studio2.0.

Table 1

Inhibitory activity of *N*-cyano-tetrahydro-pyridazine derivatives against cathepsin K, B, L and S

Compound	Structure		IC_{50}^a (nM)		
	R ₁	R ₂	B	L	K
1	-i-Propyl	-NH-Ph	53	625	25
2	-i-Propyl	-NH-Ph-(4-Cl)	110	610	24
3	-i-Propyl	-NH-Ph-(3-Cl)	32	240	11
4	-i-Propyl	-NH-Ph-(3-CF ₃)	23	48	23
5	-i-Propyl	-NH-Ph-(3-CN)	40	730	4
6	-i-Propyl	-NH-Ph-(3-CH ₃)	32	355	6
7	-i-Propyl	-NH-COO-(<i>tert</i> -Butyl)	38	130	55
8	-i-Propyl	-NH-COOCH ₂ Ph	11	145	1

^a IC_{50} values were determined from the direct regression curve analysis.

excavations by mature osteoclasts was dramatically inhibited by the treatment of compound **8** in a dose-dependent manner (Fig. 5).

In conclusion, *N*-cyano-tetrahydro-pyridazine derivatives could be developed as the specific inhibitors of cathepsin K and further used for the treatment of disorders characterized by increased bone resorption.

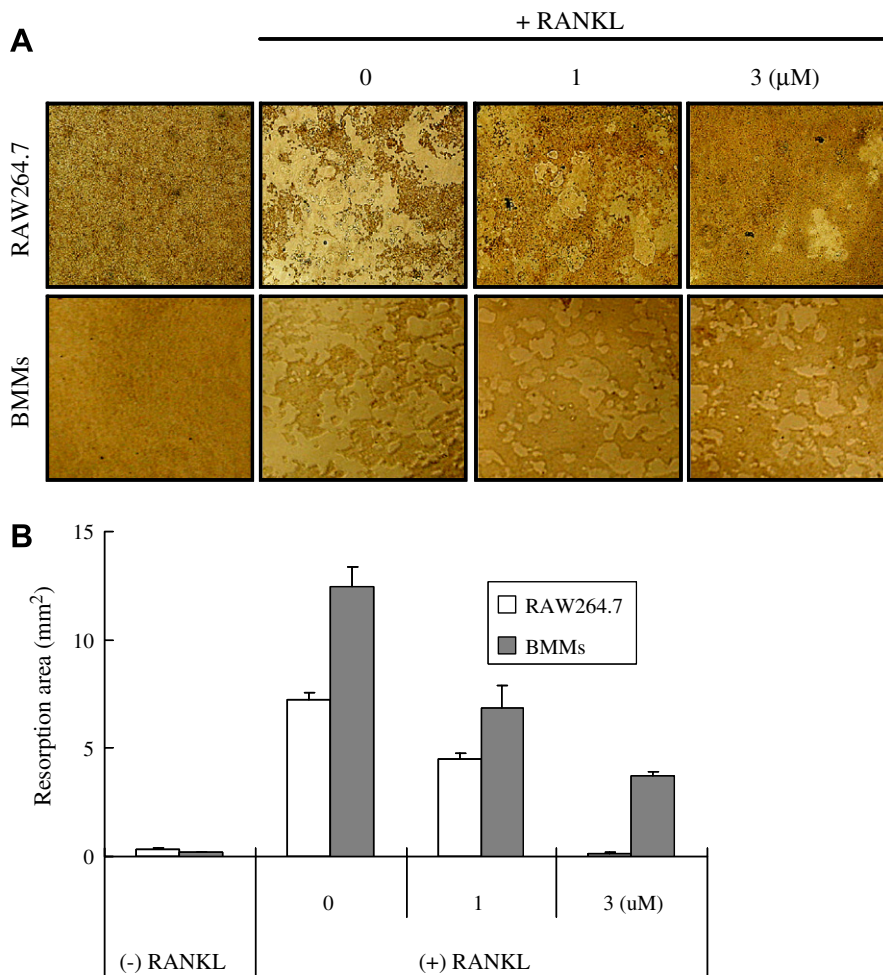


Figure 5. Effect of compound **8** on the bone resorptive activity of mature osteoclasts derived from RAW264.7 cells and BMMs. (A) The bone resorptive activity was measured by using BioCoat Osteologic mitest slides. The resorbed areas on the slides were observed under a microscope. (B) Quantification of resorbed area was performed by using Image Pro-plus program.

Acknowledgments

This research was supported by the Center for Biological Modulators of the 21st Century Frontier R&D Program, the Ministry of Science and Technology, Korea. S.H.K. and Y.K.M. were supported by the Korea Science and Engineering Foundation (KOSEF) grant funded by the Korean government (MOST) No. M10526020001-07N2602-00110.

References and notes

- Harada, S.; Rodan, G. A. *Nature* **2003**, 423, 349.
- NIH Consensus Development Panel on Osteoporosis Prevention, Diagnosis, and Therapy. *JAMA* **2001**, 285, 785.
- Rousselle, A. V.; Heymann, D. *Bone* **2002**, 30, 533.
- Troen, B. R. *Drug News Perspect.* **2004**, 17, 19.
- (a) Gelb, B. D.; Shi, G. P.; Chapman, H. A.; Desnick, R. J. *Science* **1996**, 273, 1236; (b) Yamashita, D. S.; Dodds, R. A. *Curr. Pharm. Des.* **2000**, 6, 1.
- (a) Faglueryet, J.-P.; Oballa, R. M.; Okamoto, O.; Wesolowski, G.; Aubin, Y.; Rydzewski, R. M.; Prasit, P.; Riendeau, D.; Rodan, S. B.; Percival, M. D. *J. Med. Chem.* **2001**, 44, 94; (b) Bavid, N. D.; Anne, M. H.; Robert, B. M.; Aaron, B. M.; Larry, R. M.; Lisa, M. S.; Francis, X. T.; Derril, H. W. Jr.; Lois, L. W. *Bioorg. Med. Chem. Lett.* **2005**, 15, 1815.
- Compound 1.** ¹H NMR (300 MHz, CDCl₃) δ 7.17 (m, 2H), 6.76–6.69 (m, 3H), 4.54–4.42 (m, 2H), 4.14 (d, 1H, *J* = 9.3 Hz), 3.47–3.42 (m, 1H), 3.24–2.90 (m, 2H), 2.09–1.99 (m, 2H), 1.79–1.67 (m, 2H), 1.58–1.48 (m, 1H), 1.03 (d, 3H, *J* = 6.6 Hz), 1.01 (d, 3H, *J* = 6.6 Hz); **Compound 2.** ¹H NMR (300 MHz, CDCl₃) δ 7.12 (d, 2H, *J* = 9.0 Hz), 6.63 (d, 2H, *J* = 9.0 Hz), 4.53–4.48 (m, 1H), 4.39–4.32 (m, 1H), 4.20–4.19 (m, 1H), 3.60–3.48 (m, 1H), 3.27–2.92 (m, 2H), 2.11–2.01 (m, 1H), 1.83–1.72 (m, 2H), 1.59–1.51 (m, 2H), 1.06 (d, 3H, *J* = 6.6 Hz), 1.01 (d, 3H, *J* = 6.6 Hz); **Compound 3.** ¹H NMR (300 MHz, CDCl₃) δ 7.07 (t, 1H, *J* = 8.1 Hz), 6.70–6.5 (m, 2H), 6.56 (d, 1H, *J* = 8.1 Hz), 4.54–4.40 (m, 2H), 4.29 (d, 1H, *J* = 10.2 Hz), 3.54 (m, 1H), 3.18–3.03 (m, 2H), 2.12–2.02 (m, 2H), 1.83–1.74 (m, 2H), 1.65 (m, 1H), 1.06 (d, 3H, *J* = 6.6 Hz), 1.01 (d, 3H, *J* = 6.6 Hz); **Compound 4.** ¹H NMR (300 MHz, CDCl₃) δ 7.26 (t, 1H, *J* = 7.8 Hz), 6.96 (d, 1H, *J* = 7.5 Hz), 6.85–6.83 (m, 2H), 4.53–4.42 (m, 3H), 3.56–3.52 (m, 1H), 3.18–3.01 (m, 2H), 2.17–1.95 (m, 2H), 1.83–1.73 (m, 2H), 1.56–1.52 (m, 1H), 1.09 (d, 3H, *J* = 6.6 Hz), 1.02 (d, 3H, *J* = 6.6 Hz); **Compound 5.** ¹H NMR (300 MHz, CDCl₃) δ 7.28–7.21 (m, 1H), 6.99 (d, 1H, *J* = 7.5 Hz), 6.93–6.87 (m, 2H), 4.56–4.39 (m, 3H), 3.62–3.58 (m, 1H), 3.20–3.05 (m, 2H), 2.17–2.04 (m, 2H), 1.87–1.74 (m, 2H), 1.65–1.57 (m, 1H), 1.07 (d, 3H, *J* = 6.6 Hz), 1.00 (d, 3H, *J* = 6.6 Hz); **Compound 6.** ¹H NMR (300 MHz, CDCl₃) δ 7.05 (t, 1H, *J* = 8.1 Hz), 6.57–6.49 (m, 3H), 4.54–4.44 (m, 2H), 4.13 (m, 1H), 3.69–3.44 (m, 1H), 3.29–2.92 (m, 2H), 2.26 (s, 3H), 2.10–1.99 (m, 2H), 1.79–1.48 (m, 3H), 1.05 (d, 3H, *J* = 6.6 Hz), 1.00 (d, 3H, *J* = 6.6 Hz); **Compound 7.** ¹H NMR (300 MHz, CDCl₃) δ 5.02 (d, 1H, *J* = 9.0 Hz), 4.73–4.68 (m, 1H), 4.51 (d, 1H, *J* = 9.9 Hz), 3.60–3.52 (m, 2H), 3.18–3.10 (m, 1H), 2.13–2.01 (m, 2H), 1.99–1.84 (m, 2H), 1.80 (m, 1H), 1.43 (s, 9H), 1.03 (d, 3H, *J* = 6.6 Hz), 0.93 (d, 3H, *J* = 6.6 Hz); **Compound 8.** ¹H NMR (300 MHz, CDCl₃) δ 7.36–7.34 (m, 5H), 5.28 (d, 1H, *J* = 9.6 Hz), 5.15–5.03 (m, 2H), 4.78–4.75 (m, 1H), 4.51 (d, 1H, *J* = 12.0 Hz), 3.53–3.50 (m, 2H), 3.20–3.11 (m, 1H), 2.06–1.99 (m, 2H), 1.83–1.79 (m, 1H), 1.04 (d, 3H, *J* = 6.6 Hz), 0.93 (d, 3H, *J* = 6.9 Hz).
- Eldridge, M. D.; Murray, C. W.; Auton, T. R.; Paolinine, G. V.; Mee, R. P. *J. Comput. Aided Mol. Des.* **1997**, 11, 425.
- Biological activity assay: **In vitro enzymatic activity assay for cathepsin B, L, and K.** The enzymatic reaction was performed in a 96-well plate (Costar) by mixing reaction buffer (100 mM NaOAcetate, 2 mM EDTA, 3 mM DTT, pH 5.5), 5 μl of 400 μM substrate (Z-RR-PNA; biomol), 5.88 nM recombinant human cathepsin B (1–339 amino acid), and 5% (v/v) compound (12.5 mM DMSO stock solution used). The mixture was incubated at 30 °C for 2 h, and then its absorbance was measured at 405 nm in Benchmark plus (Bio-Rad). The substrates Z-FR-pNA and Z-GPR-AMC (biomol) were used in assay for cathepsin L and K, respectively. In addition, 300 mU recombinant cathepsin L

(Calbiochem) and 20 nM recombinant human cathepsin K (1–329 amino acid) were used in each assay. **Cell culture and induction of multinucleated osteoclasts.** Osteoclast generation was achieved using either mouse monocyte/macrophage RAW264.7 cells or the primary cultures of mouse BMMs with modifications. RAW264.7 cells were purchased from American Type Culture Collection and maintained in Dulbecco's Modified Eagle's Medium (DMEM, HyClone, UT) supplemented with 10% fetal bovine serum (FBS, HyClone), 100 U/ml of penicillin, and 100 mg/ml streptomycin with a change of medium every 3 days in humidified atmosphere of 5% CO₂ at 37 °C. In order to differentiate osteoclasts, RAW264.7 cells were suspended in α -minimal essential medium (α MEM, HyClone) supplemented with 10% FBS and 100 ng/ml RANKL (R&D Systems Inc., MN), and plated in a 96-well plate at the density of 1×10^3 cells/well. Then, after 3–4 days, multinucleated osteoclasts were observed. For the generation of bone marrow-derived osteoclasts, monocytes were isolated from femur and tibiae of BALB/c mice (Central Lab. Animal Inc., Korea), seeded, and cultured in α MEM with 10% FBS and 10 ng/ml macrophage colony stimulating factor (M-CSF; R&D Systems Inc.) for 1 day. Suspended cells at this stage were considered M-CSF-dependent BMMs and used as osteoclasts precursors. Induction of differentiation to osteoclasts was achieved by culturing those

cells plated into a 96-well plate at the density of 3×10^3 cells/well in α MEM with 10% FBS, 100 ng/ml RANKL, and 30 ng/ml M-CSF. Multinucleated osteoclasts were observed on the differentiation day 6. **Pit formation assay.** RAW264.7 cells were suspended in α MEM with 10% FBS and 100 ng/ml RANKL, and plated on BioCoat Osteologic multitest slides (BD Biosciences, MA), which were coated with submicron synthetic calcium phosphate thin films, at the density 1×10^3 cells/well. The medium was replaced with a fresh one every 3 days. Multinucleated osteoclasts were observed from the differentiation day 3, and at that time, compound **8** was treated into multinucleated osteoclasts derived from RAW264.7 cells. After the incubation for 3 days, the slides were washed with 6% sodium hypochloride solution to remove cells. The resorbed areas on the slides were observed under a microscope. M-CSF-dependent BMMs were plated and cultured in α MEM with 10% FBS, 100 ng/ml RANKL, and 30 ng/ml M-CSF. The medium was replaced with a fresh one every 3 days. Multinucleated osteoclasts were observed on the differentiation day 6, and at that time, compound **8** was added every 3 days. On the differentiation day 15, the slides were washed and observed as described above. This experiment was performed in triplicate. Quantification of resorbed area was performed by using Image Pro-plus program, version 4.0 (Media Cybernetics Inc., MD).